

NUMERICAL STUDY ON THE EFFECT OF RAINWATER EVAPORATION ON SEVERE CONVECTIVE WEATHER UNDER DIFFERENT BOUNDARY LAYER PARAMETERIZATION SCHEMES

Tang Jie, Liu Xiaoli

Nanjing University of Information Science and Technology, Key Laboratory of aerosol and cloud precipitation in China Meteorological Administration, Nanjing, Jiangsu 210044
(Received January 07 2018, accepted May 25 2018)

Abstract Three boundary layer parameterization schemes (MRF,UW,YSU) in mesoscale numerical model (WRF) are used to simulate a severe convective weather in Zhejiang on November 9, 2009 without considering the rainwater evaporation term and considering the rainwater evaporation term. The numerical simulation results of macroscopic and microscopic physical mechanisms of strong convection were compared. The results show that without considering the evaporation of rainwater, the rainbands simulated by the three boundary layer schemes are narrower, hourly precipitation is smaller, convective monomer moves slower, and the precipitation overlap area is more. The simulated radar reflectivity intensity is significantly reduced and the echo band is narrower. Whether rain evaporation is considered or not, the YSU scheme simulates the strongest precipitation and radar reflectivity, MRF scheme is close to it and the UW scheme is the weakest. By analyzing the macro conditions of convection development, it can be seen that under the condition of considering the rainwater evaporation, high and low altitude divergence configuration simulated by the three boundary layer schemes is better, the water vapor transport is more abundant, updraft and downdraft are stronger, providing more favorable conditions for the occurrence and development of strong convection. Whether rain evaporation is considered or not, the water vapor conditions and high and low altitude divergence configuration simulated by the YSU scheme are better, results simulated by MRF scheme is similar to YSU scheme. The convection generation condition simulated by the UW scheme is the weakest of the three schemes. Under the condition of considering the rainwater evaporation, more hydrotal particles simulated by three boundary layer schemes, and stronger updraft, which is more conducive to development of convection. Whether rain evaporation is considered or not, the MRF and YSU schemes can simulate more rain, mainly because the vertical movement of the airflow is stronger, and more cloud water becomes cold cloud water under the strong ascending airflow, and more cold water frozen with graupel to form graupel, graupel melts to produce more rain. The UW scheme have poor macroscopic conditions, and the updraft is weaker. Cold cloud water is less, and cold cloud water and graupel are less frozen, resulting in less rainwater content

Keywords: mesoscale numerical model, boundary layer parameterization scheme

1. Introduction

The boundary layer scheme is an important part of the study of physical parameterization schemes in numerical models(Morrison et al. 2008;Aksoy et al. 2006;Deng et al. 2006). The selection of boundary layer parameterization schemes in the model has a significant impact on the simulation results of strong convection processes(Jankov et al. 2004;Nielsengammon et al.2010). Many scholars have successively made relevant researches to show that under the same circumstances, the ability of the boundary layer scheme to predict precipitation is not the same(Zhang et al. 2013;Zhou et al. 2013). Introducing a reasonable boundary layer parameterization scheme can effectively improve the ability of numerical models to simulate strong convective weather(Wang et al. 2010;Cai et al. 2007).

In recent years, research on cloud microphysical structures has become an important means of understanding the process of strong convection(Doswell et al. 1987).The phase change of water is an important part of the study of cloud microphysical structure. The phase change of water in strong convection process, especially the evaporation process, melting process and latent heat change caused by sublimation process are the main causes of vertical airflow field change(Li et al. 2013). Many scholars use numerical models to explore this, and believe that the latent heat change caused by evaporation process is the main influence factor of vertical flow field and convective cloud system characteristics change in cloud(Yang et al. 2009). Through analysis, it is found that precipitation occurs due to evaporation, which causes the amount of supercooled water in the cloud to decrease(Wang et al. 2002). Discuss the relationship between microphysical processes such as rainwater evaporation process and latent heat, and find that the rainwater evaporation process is the main cause of the downdraft(Fernández-González et al. 2016), the low-level sinking airflow is mainly generated by the melting

process and the evaporation process(Liu et al. 2010),and the evaporation process and the melting process in the convective system increase the instability of the convective system(Braun et al. 2010).

Based on this, this paper uses three different boundary layer parameterization schemes (MRF, UW, YSU) to simulate a strong convective weather process in Zhejiang, and discusses the impact of rainwater evaporation on this case from macroscopic and microscopic perspectives.

2. Observations and model

a. Observations

On November 9, 2009, there was strong convective weather in Zhejiang Province. At 08:00 (UTC), south trough is located in the south of China at 500 hPa, and the temperature trough after the height trough, will continue to move eastward and deepen,and affect the Zhejiang area. At 700 hPa, low-level jet stream in the south of the Yangtze River valley transport warm and humid air, accompanied by strong convergence of water vapor at the front. At 850 hPa, the shear line above the Yangtze River vally promotes air convergence and elevation.And the temperature ridge is located in the coastal area,under the southwesterly airflow, warm air is transported to the north. The cold air on the ground is transported southward under the guidance of the northwest airflow.This high and low altitude configuration is very conducive to the development of strong convective weather in Zhejiang.(Fu et al. 2016).

b. Introduction of simulation scheme

In this paper, WRF v3.4 mesoscale model is used for numerical simulation. The initial field and the lateral boundary field are provided by using the NECP global reanalysis data (1×1) every 6 hours. The longitude and latitude of the simulation center for the severe convection weather process is 29.6° N , 119.8° E. The integration time of the model is 00:00 (UTC) on November 9, 2009, the integral time is 12 hours, the step length is 36s; the two nesting of the model is used. The grid spacing is 6 km, 2 km, the second grid number is 262×280 , the output time is 30mins and 10 mins, the model is divided into 27 layers in the vertical direction, and the top pressure is 100hPa. The topographic data are the global 5 m and 2m topographic data of U.S. Geological Survey. The region of this simulation is shown in figure 1. With the exception of the boundary layer parameterization schemes (MRF, UW, YSU), the other parameter schemes of the two regions are designed with the same scheme (Table 1).Under the conditions of different boundary layer parameterization schemes, the rainwater evaporation s are turned on and off respectively, and then numerical simulations are carried out for this case.

Table 1 Schemes selected in this study

Microphysical scheme	MY
Land surface process scheme	Noah
Near-surface layer scheme	MYJ Monin-Obukhov
Long wave radiation scheme	RRTM
Shortwave radiation scheme	Dudhia
Cumulus convection parameterization scheme	Kain-Fritsch(new Eta)

3. Results

a. Surface precipitation analysis

Figure 2 shows the 12-hour cumulative precipitation simulated by the three boundary layer parameterization schemes without considering the rainwater evaporation term (top) and considering the rainwater evaporation term (bottom).In any case, the simulated cumulative precipitation is higher than the actual measurement. Under considering rainwater evaporation, the cumulative precipitation simulated by UW scheme is the closest to the actual situation. Moreover, it can be seen that without considering the rainwater evaporation term, local cumulative precipitation is significantly increased simulated by the three boundary layer parameterization schemes at the junction of Anhui and Anhui, and the rain belt is narrow. The

accumulated precipitation of the YSU boundary layer scheme is the largest whether rain evaporation is considered or not.

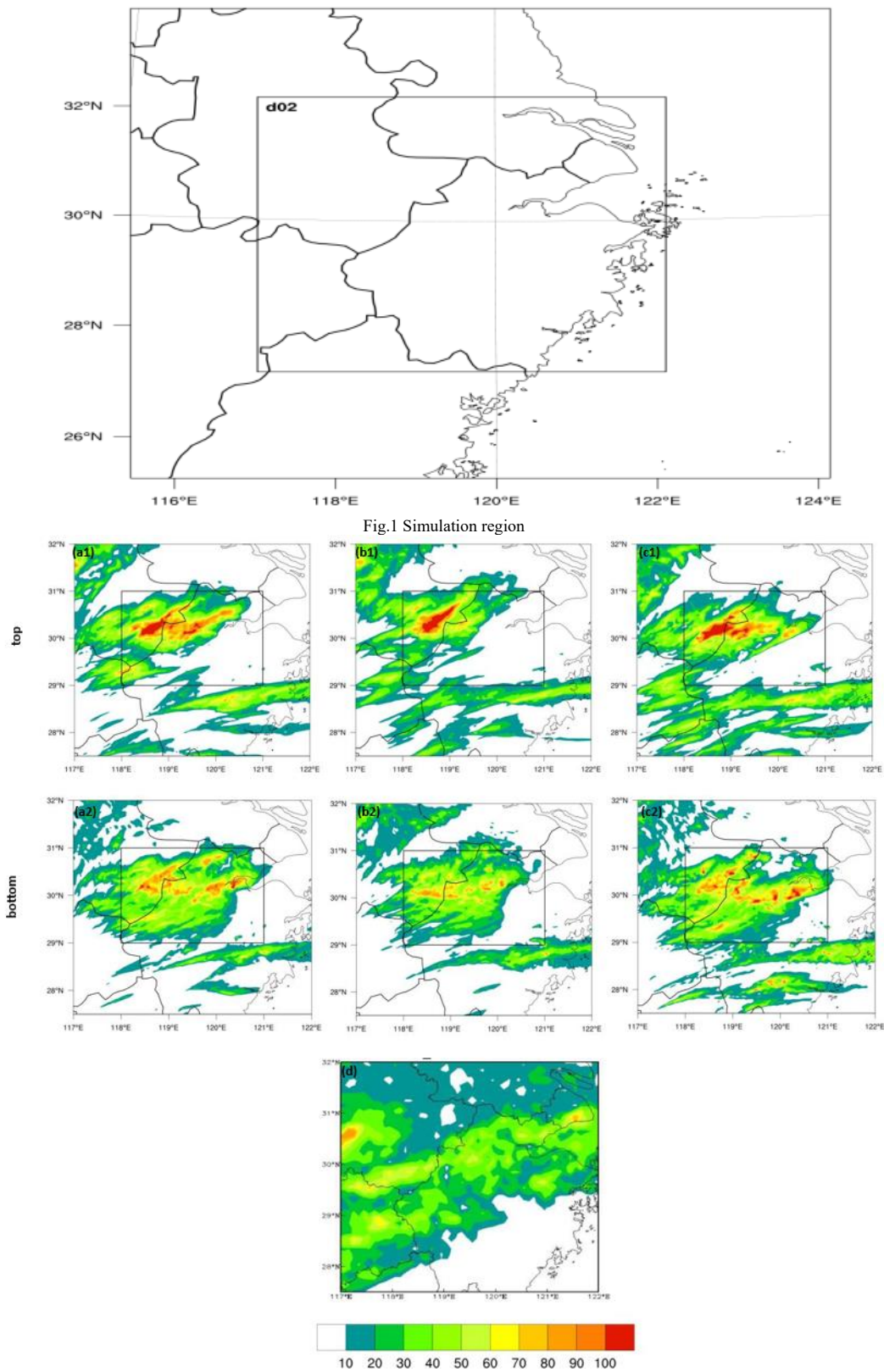


Fig. 2 12-hour cumulative precipitation simulation on november 9, 2009 without considering the rainwater evaporation term (top) and considering the rainwater evaporation term (bottom), (a)MRF; (b)UW; (c)YSU;(d)CMORPH

Figure 3 and Figure 4 show the hourly cumulative precipitation simulated by the three boundary layer parameterization schemes without considering the rainwater evaporation term (top) and considering the rainwater evaporation term (bottom). In the case of without considering the rainwater evaporation term, the hourly precipitation simulated by the three boundary layer parameterization schemes is smaller, the moving speed of the rain belt is slower, and there are more precipitation overlapping areas at two times, which results in the local 12-hour cumulative precipitation was too large in the junction of Anhui and Zhejiang. In the three boundary layer parameterization schemes, the YSU scheme simulates the largest amount of hourly precipitation, whether rain evaporation is considered or not.

b. Characteristic of radar reflectivity

Figure 5 shows radar reflectivity at the mature stage simulated by three kinds of boundary layer parameterization schemes without considering the rainwater evaporation term (top) and considering the rainwater evaporation term (bottom). The simulation results show that the radar reflectivity intensity simulated by the three boundary layer parameterization schemes without considering the rainwater evaporation term is obviously weakened, and the echo band is narrower. In addition, whether rain evaporation is considered or not, the MRF and YSU schemes can better simulate another strong echo area on the east side of the echo belt. Compared with the results simulated by UW scheme, the intensity of the radar reflectivity in the mature stage simulated by the MRF and YSU schemes are stronger.

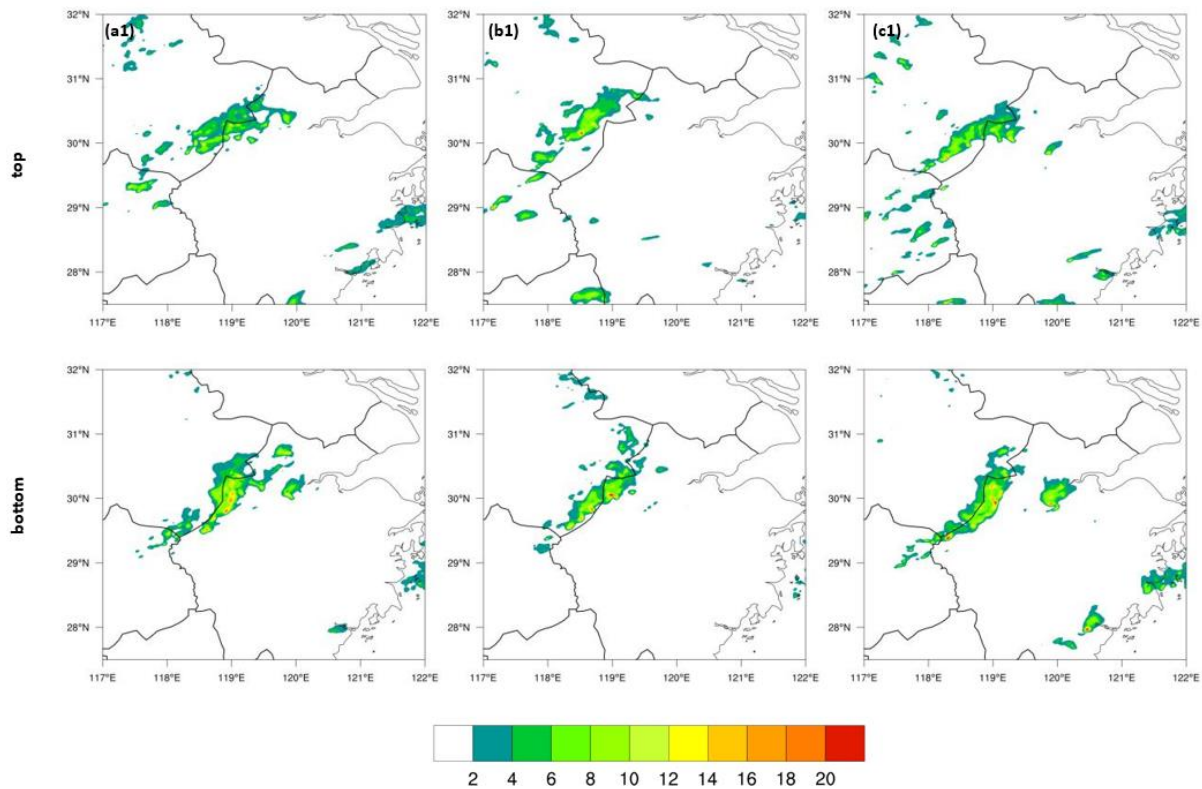


Fig. 3 1-hour cumulative precipitation simulation at 9:00 without considering the rainwater evaporation term (top) and considering the rainwater evaporation term (bottom), (a)MRF; (b)UW; (c)YSU

4. Macroscopic characteristics

a. Water vapor flux divergence

Figure 6 shows the low-level water vapor flux divergence in the mature stage simulated by the three boundary layer parameterization schemes without considering the rainwater evaporation term (top) and considering the rainwater evaporation term (bottom). The results show that the water vapor flux divergence simulated by the three boundary layer parameterization schemes is stronger after considering the rainwater evaporation, and can provide more water vapor for the development of convection. The water vapor convergence intensity simulated by the MRF and YSU schemes is stronger whether considering rainwater evaporation or not. And the water vapor convergence intensity is weaker simulated by UW scheme.

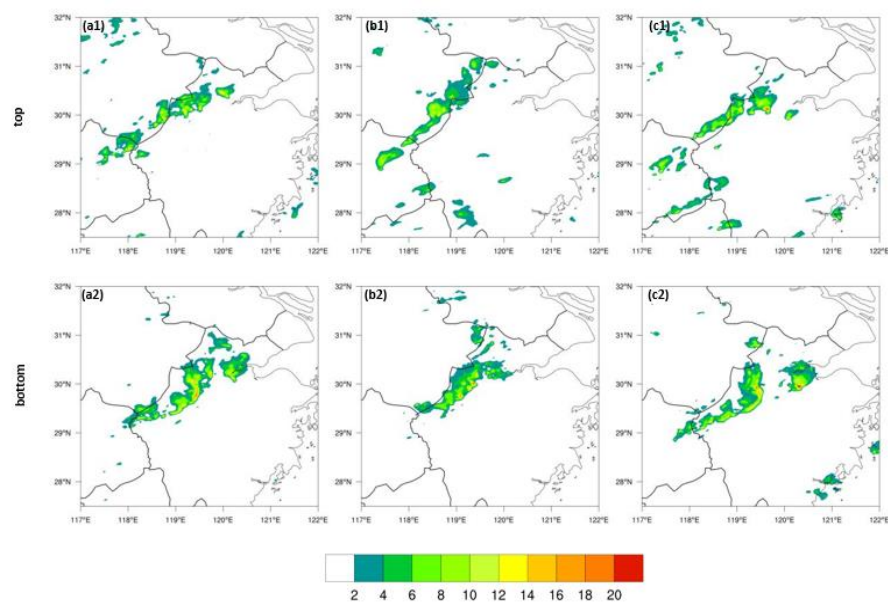


Fig. 4 1-hour cumulative precipitation simulation at 10:00 without considering the rainwater evaporation term (top) and considering the rainwater evaporation term (bottom) (a)MRF; (b)UW; (c)YSU

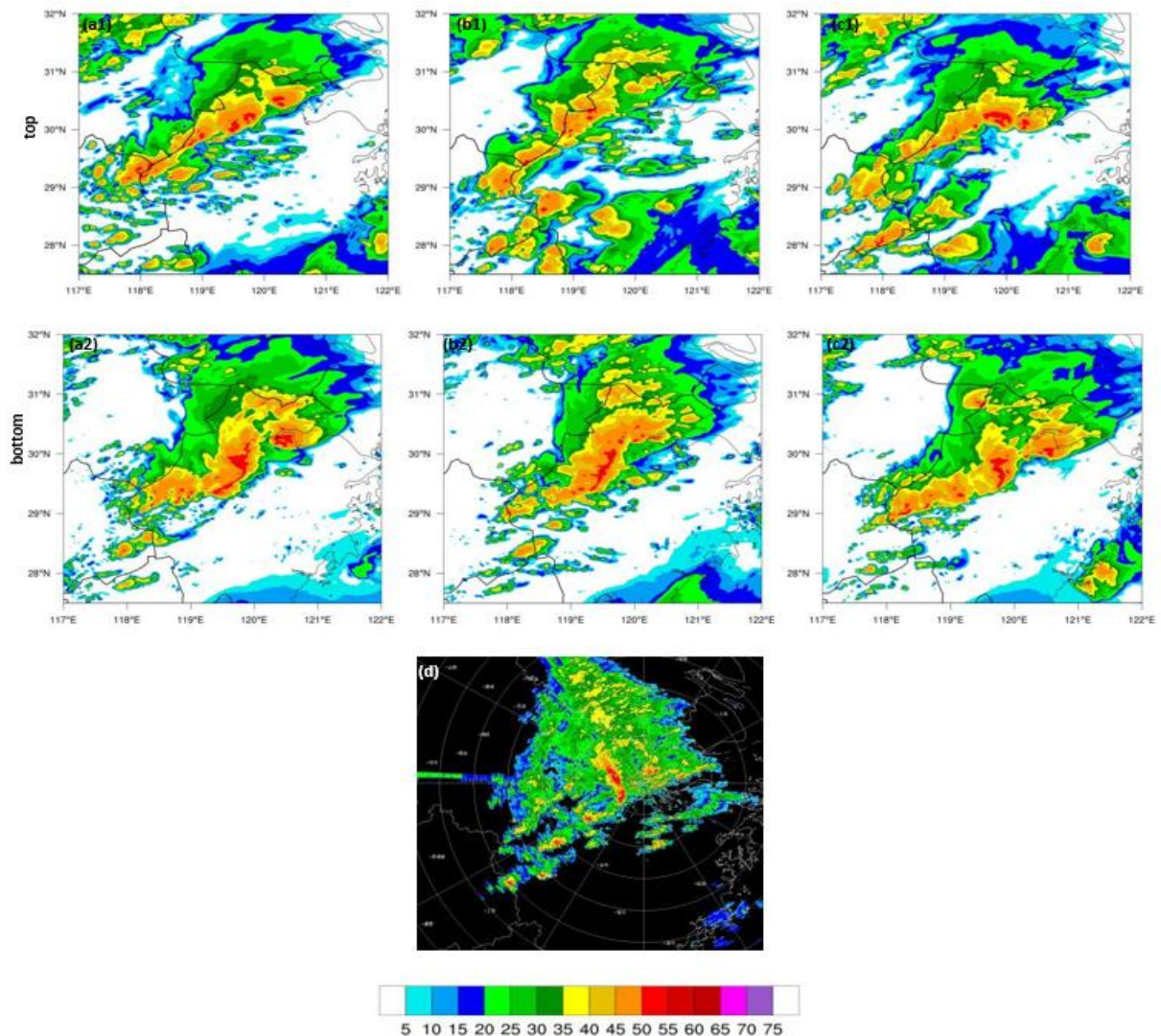


Fig. 5 radar reflectivity at the maturity stage without considering the rainwater evaporation term (top) and considering the rainwater evaporation term (bottom), (a)MRF; (b)UW; (c)YSU;(d)Observation

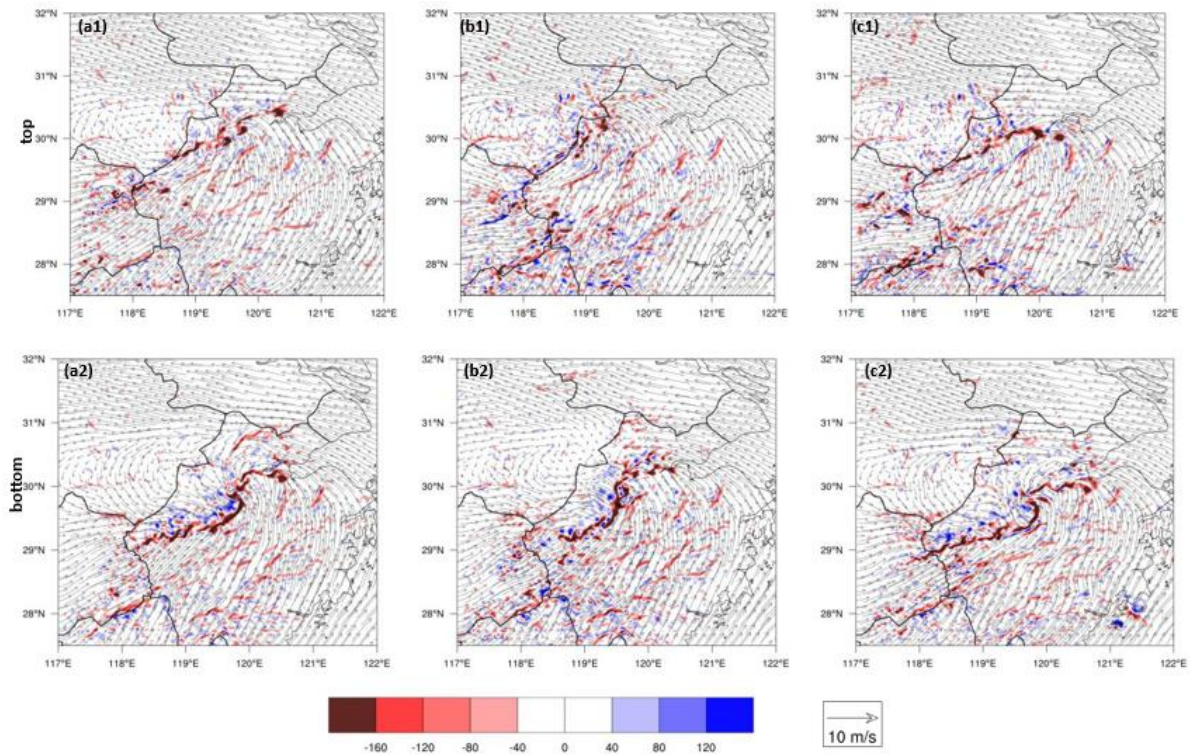


Fig. 6 Water vapor flux divergence at the maturity stage without considering the rainwater evaporation term (top) and considering the rainwater evaporation term (bottom) (a)MRF; (b)UW; (c)YSU

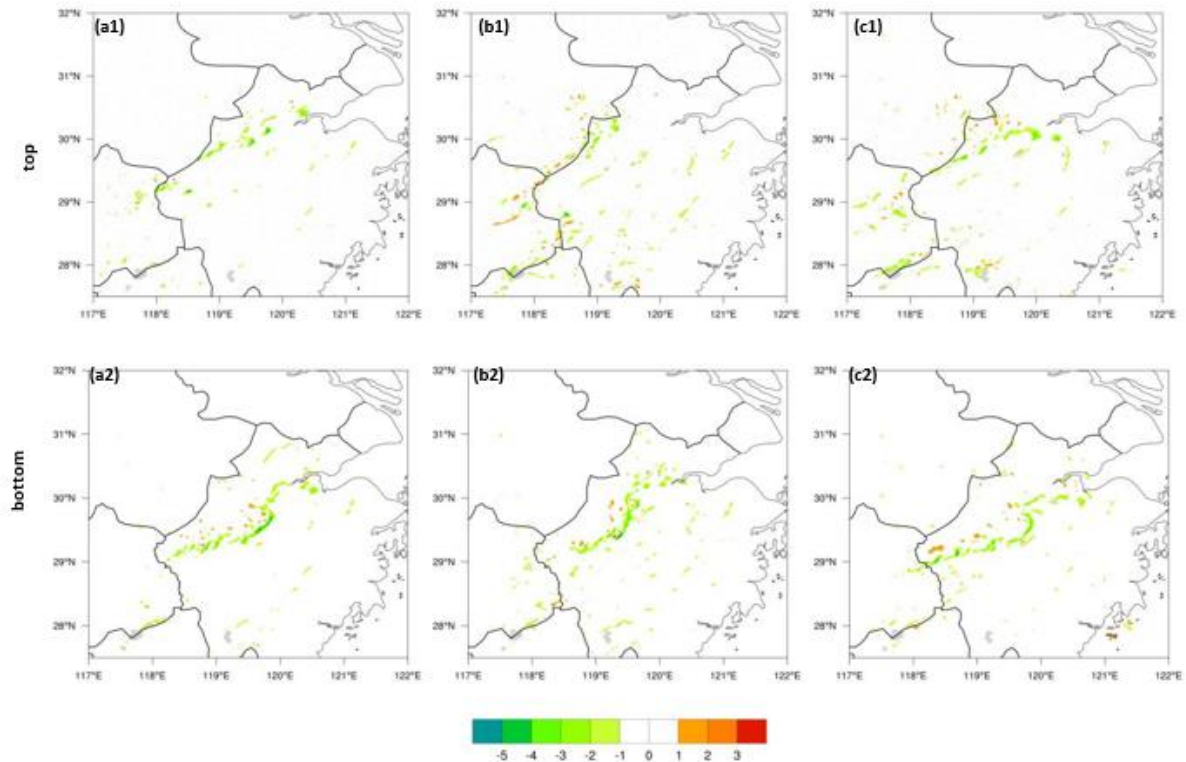


Fig. 7 850hPa-convergent field at the maturity stage without considering the rainwater evaporation term (top) and considering the rainwater evaporation term (bottom) (a)MRF; (b)UW; (c)YSU

b. Divergence field

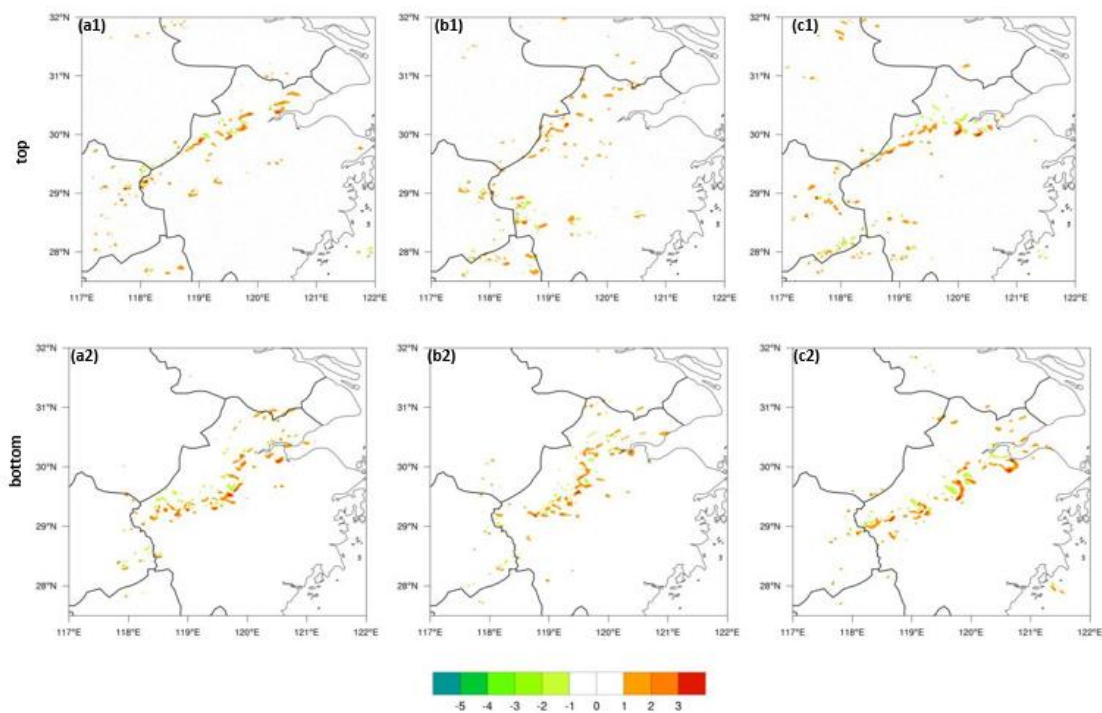


Fig. 8 500hPa-divergent field at the maturity stage without considering the rainwater evaporation term (top) and considering the rainwater evaporation term (bottom) (a)MRF; (b)UW; (c)YSU

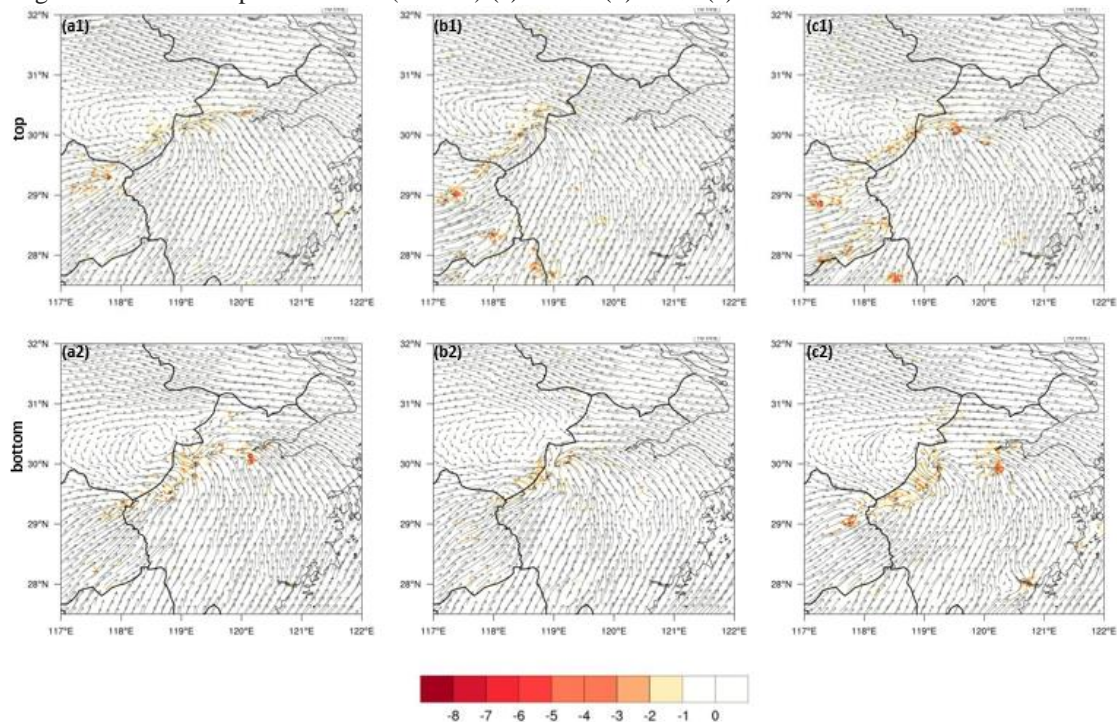


Fig. 9 Strongest downdraft in the mature stage simulated by three boundary layer parameterization schemes without considering the rainwater evaporation term (top) and considering the rainwater evaporation term (bottom) (a)MRF; (b)UW; (c)YSU

Figure 7 and Figure 8 show the divergence field in the mature stage simulated by three boundary layer parameterization schemes without considering the rainwater evaporation term (top) and considering the rainwater evaporation term (bottom). In the case of considering the evaporation of rainwater, both the low-level convergence and the high-level divergence are strong, and the high-low-altitude configuration is better, which makes the air ascending motion stronger and facilitates water vapor accumulation and upward transportation. Whether rain evaporation is considered or not, the high and low divergence simulated by the

YSU and MRF schemes are stronger. The high and low divergent fields simulated by the UW scheme are the weakest, so airflow vertical ascending motion simulated by this scheme is weaker and the water vapor upward transport conditions are not as good as the YSU and MRF schemes.

c. Strongest downdraft

Figure 9 show strongest downdraft in the mature stage simulated by three boundary layer parameterization schemes without considering the rainwater evaporation term (top) and considering the rainwater evaporation term (bottom). Under the condition of considering the evaporation of rainwater, the downdraft flow simulated by the three schemes is obviously larger, which may be due to the fact that in this case, the latent heat absorption is larger and the convective temperature is significantly lower, making the sinking airflow more exuberant. Whether rain evaporation is considered or not, the downflow airflow simulated by the YSU and MRF schemes is strong, and the sinking airflow simulated by the UW scheme is the weakest.

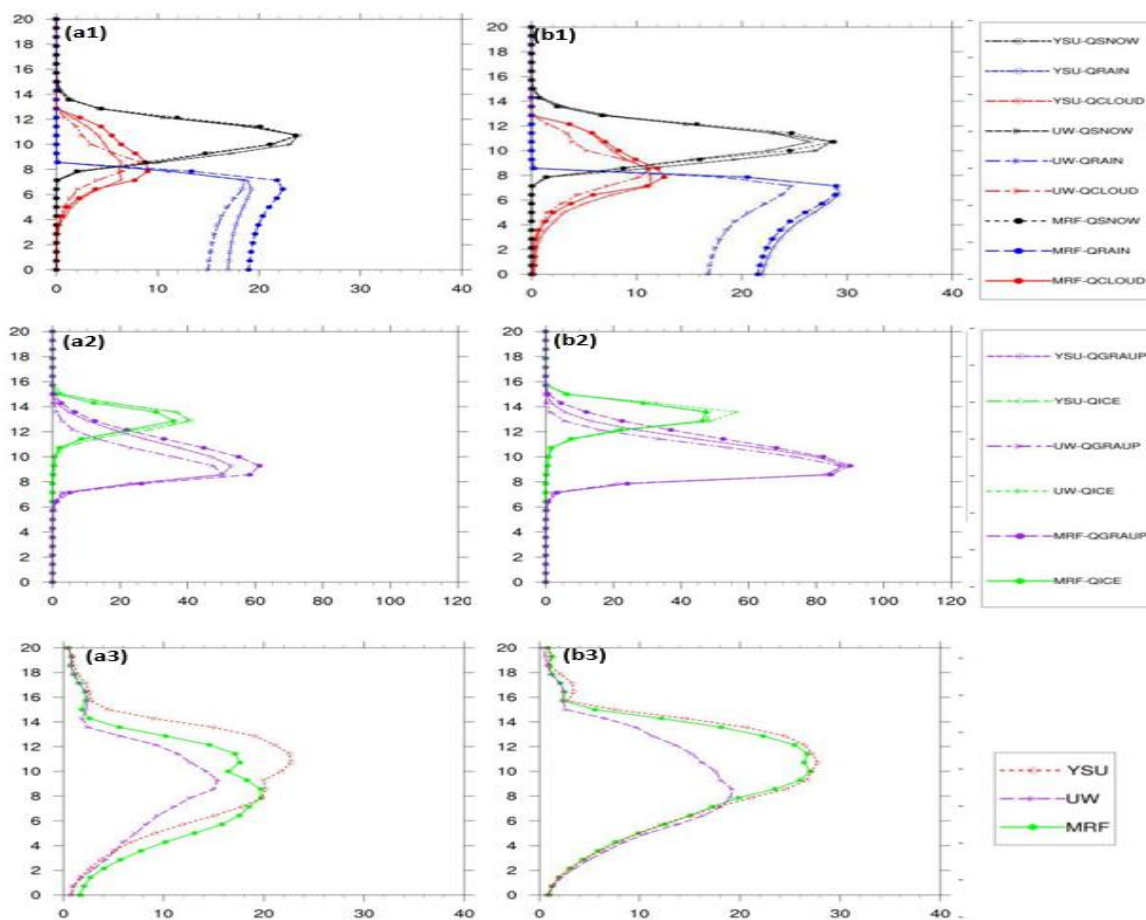


Fig. 10 Average vertical distribution of snow (black), rain (blue), cloud water (red), ice crystal (green), graupel (purple) at the maturity stage and maximum updraft vertical distribution. Solid Dots: MRF. Hollow Dots: YSU. Triangle: UW.

5. Cloud microphysical structure

Figure 10 shows the vertical profile of the average area of the hydrometeor particles and the maximum updraft, simulated by three boundary layer parameterization schemes, without considering rainwater evaporation (a1~a3) and considering the rainwater evaporation (b1~b3). It can be seen from the figure that under the conditions of considering the rainwater evaporation, the content of various hydrometeor particles simulated by the three schemes is increased, and the mutual conversion efficiency between the particles is higher, resulting in more rain. In addition, under the condition of considering the rainwater evaporation, the updraft at each height simulated by the three schemes is obviously stronger, and the height of the strongest ascending airflow is obviously higher, indicating that the convection development is more vigorous. Whether rain evaporation is considered or not, the vertical ascending airflow simulated by the MRF and YSU schemes in the three schemes is stronger, and the content of each of the water-forming particles is larger, and more cloud water is formed.

into a cold cloud water under the strong ascending airflow. More cold clouds and graupel freezes to form graupel, which melts and produces more rain. However, the UW scheme simulates a weaker updraft, and the amount of cloud water that is transported above the zero-degree layer is small, and cold water and graupel are less frozen, resulting in less rain.

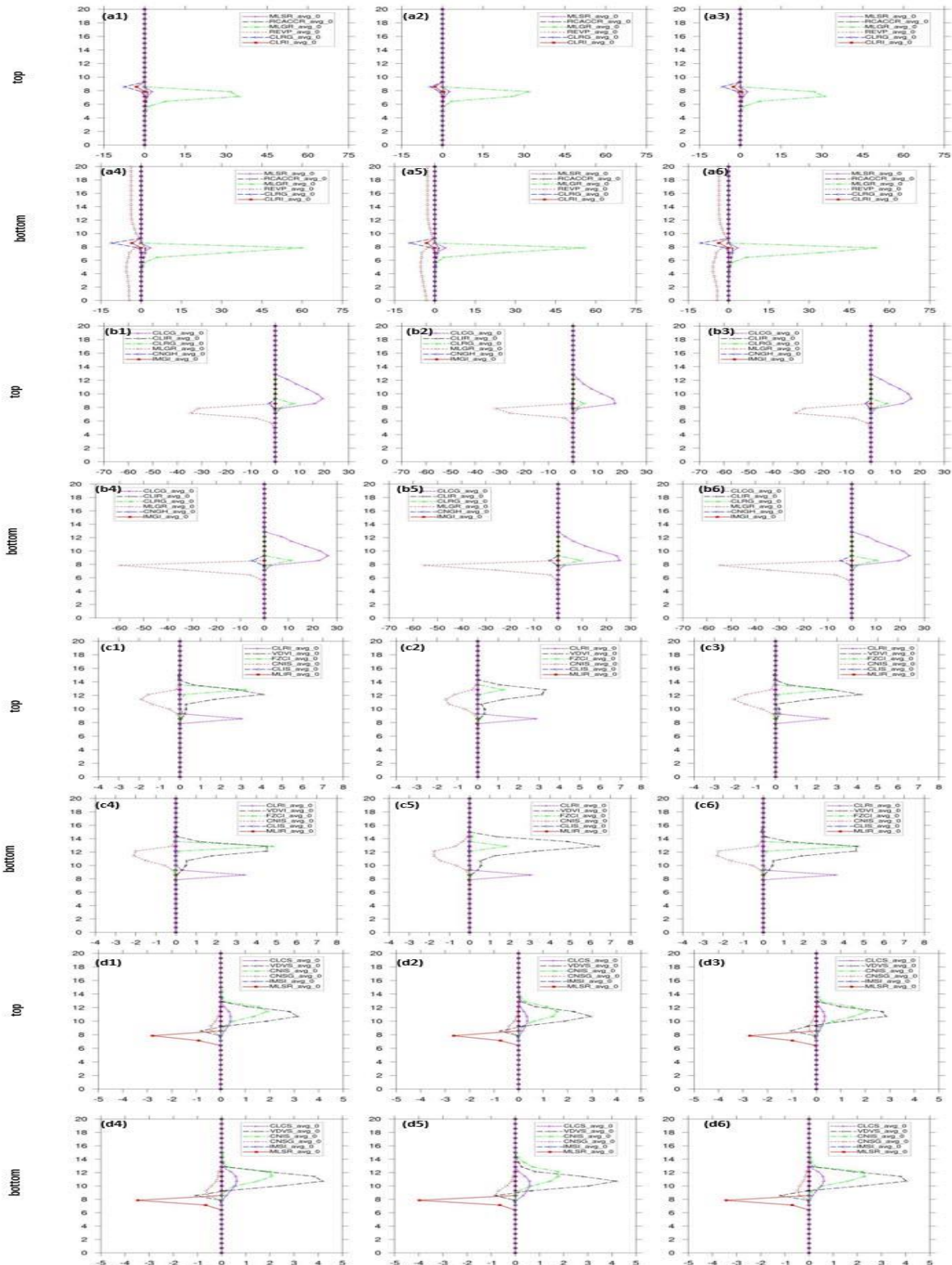


Fig. 11 Vertical distribution of average source and sinks in rainwater (a), strontium (b), ice crystal (c), and snow (d) regions without considering the rainwater evaporation term (top) and considering the rainwater evaporation term (bottom) 1 and 4: MRF 2 and 5: UW 3 and 6: YSU

6. Conclusion

- (a) The simulation results show that under the condition of without considering evaporation of rainwater, the rainbands simulated by the three boundary layer schemes are narrower, the hourly precipitation is smaller, and the convective monomer move slower, resulting in precipitation overlap area is more. Under these circumstances, the radar reflectivity intensity simulated by the three boundary layer parameterization schemes is obviously weaker, and the echo band is narrower. In addition, whether rain evaporation is considered or not, the YSU scheme simulates the highest precipitation and radar reflectivity. The simulation result of the MRF scheme is closer to the YSU scheme, but the simulated precipitation and strong echo centers are relatively dispersed. The precipitation intensity and radar reflectivity intensity simulated by the UW scheme are the weakest.
- (b) Under the condition of considering the rainwater evaporation, high and low altitude divergence configuration simulated by the three boundary layer schemes is better, the water vapor transport is more abundant, updraft and downdraft are stronger, convective conditions are more unstable, providing more favorable conditions for the occurrence and development of strong convection, which is the macroscopic cause for the convective monomer moving faster and producing more precipitation. Regardless of whether the rainwater evaporation is considered or not, the three boundary layer parameterization schemes (MRF, UW and YSU) have significant effects on the simulation results. The water vapor conditions and high and low altitude divergence configuration simulated by the YSU scheme are better, and the result simulated by MRF scheme is similar to that of YSU scheme. The convection generation condition simulated by the UW scheme is the weakest. This is the macro reason for less precipitation simulated by this scheme.
- (c) It can be seen from the cloud microphysical structure that considering the rainwater evaporation, more hydrometeor particles simulated by three boundary layer schemes, and stronger updraft, which is more conducive to development of convection. Whether rain evaporation is considered or not, the MRF and YSU schemes can simulate more rain, mainly because the vertical movement of the airflow is stronger, and more cloud water becomes cold cloud water under the strong ascending airflow, and more cold water frozen with graupel to form graupel, graupel melts to produce more rain. The UW scheme have poor macroscopic conditions, and the updraft is weaker. Cold cloud water is less, and cold cloud water and graupel are less frozen, resulting in less rainwater content.

7. Reference

- [1] Aksoy A, Zhang F, Nielsen-Gammon J W. Ensemble-based simultaneous state and parameter estimation with MM5. *Geophysical Research Letters*, 2006, 33(12):347-366.
- [2] Braun S A, Houze R A. Melting and freezing in a mesoscale convective system. *Quarterly Journal of the Royal Meteorological Society*, 2010, 121(121):55-77.
- [3] Cai Xiang-ning, Zhou Qingliang, Zhong Qing, et al. Influence of boundary layer parameterization on the numerical simulation of precipitation in "Ya'an Tian-leakage". *Meteorology*, 2007YIAN33 (5): 12-19.
- [4] Doswell C A I. The Distinction between Large-Scale and Mesoscale Contribution to Severe Convection: A Case Study Example. *Weather & Forecasting*, 1987, 2(1):3-16.
- [5] Deng A, Stauffer D R. On improving 4-km mesoscale model simulations. *Journal of applied meteorology and climatology*, 2006, 45(3):361-381.
- [6] Fernández-González S, Wang P K, Gascón E, et al. Latent cooling and microphysics effects in deep convection. *Atmospheric Research*, 2016, 180:189-199.
- [7] Fu Y, Liu X L, Ding W. Numerical simulation of a hail process and the physical structure of the cloud. *Journal of Tropical Meteorology*, 2016, 32(4):546-557.
- [8] Jankov I, Gallus W A, Shaw B, et al. An investigation of IHOP convective system predictability using a matrix of 19 WRF members//20th Conference on Weather Analysis and Forecasting/16th Conference on Numerical Weather Prediction. 2004, 10-15.
- [9] Li R, Min Q, Wu X, et al. Retrieving latent heating vertical structure from cloud and precipitation profiles—Part II: Deep convective and stratiform rain processes. *Journal of Quantitative Spectroscopy & Radiative Transfer*, 2013, 122(6):47-63.
- [10] Liu C, Moncrieff M W, Zipser E J. Dynamical Influence of Microphysics in Tropical Squall Lines: A Numerical Study. *Monthly Weather Review*, 2010, 125(9):2193.
- [11] Morrison, Thompson H G, Tatarskii V. Impact of cloud microphysics on the development of trailing stratiform precipitation in a simulated squall line: Comparison of one- and two-moment schemes. Submitted to *Monthly Weather Review*, 2008, 1(1):991-1007.
- [12] Nielsengammon J W, Hu X M, Zhang F, et al. Evaluation of Planetary Boundary Layer Scheme Sensitivities for the

- Purpose of Parameter Estimation. *Monthly Weather Review*, 2010, 138(9):3400-3417.
- [13] Wang Ying, Zhang Rum, Hu Ju, et al. Tests of the WRF model on the simulation ability of the urban boundary layer in the valley and analysis of the surface meteorological characteristics. *Plateau Meteorology*, 2010: 29 (6): 1397-1407.
- [14] Wang P. Numerical Study on Cloud Physical Processes of Heavy Rainfall in South China. *Quarterly Journal of Applied Meteorology*, 2002(1):78-87.
- [15] Yang M H, Houze R A. Sensitivity of Squall-Line Rear Inflow to Ice Microphysics and Environmental Humidity. *Monthly Weather Review*, 2009, 123(11):3175.
- [16] Zhang Xiaopei, Yin Y. Evaluation of four boundary layer parameterization schemes for WRF model in complex terrain areas. *Acta Atmospheric Science*, 2013N 36 (1): 68-76 .
- [17] Zhou Qiang, Li Guoping. Effects of boundary layer parameterization scheme on the simulation of the eastward movement of the plateau vortex. *Plateau Meteorology*, 2013Y32 (2): 334-344 .

